Open Access

Recent Progress in Materials

Research Article

Evaluating the Performance of Hollow Core Slabs (HCS)-Concrete and Simplifying Their Implementation

Amir Mahboob [1,*], Omid Hassanshahi [2], Abdulqaiyoum Hakimi [3], Mohammad Safi [4]

1. Strength of Materials and Structural Engineering Department, Polytechnic University of Catalonia, C/Colom 11, TR45, 08222 Terrassa, Spain; E-Mail: amir.mahboob@upc.edu
2. Department of Civil Engineering, ISISE, University of Minho, Campus de Azurém, 4800-058 Guimarães, Portugal; E-Mail: omid.hasanshahi@civil.uminho.pt
3. Ghalib University, West of Park Taraqi, Hanzala Badghisi Road, Herat, Afghanistan; E-Mail: abdulqaiyoum.hakimi@gmail.com
4. Faculty of Civil, Water and Environmental Engineering, Shahid Beheshti University, Tehran, Iran; E-Mail: m_safi@sbu.ac.ir

* **Correspondence:** Amir Mahboob; E-Mail: amir.mahboob@upc.edu

Academic Editor: Mostafa Seifan

Special Issue: New Trends on Construction Technologies and Sustainable Building Materials

Recent Progress in Materials
2023, volume 5, issue 2
doi:10.21926/rpm.2302016

Received: March 02, 2023
Accepted: April 11, 2023
Published: April 19, 2023

Abstract

The largest proportion of the material used in multistory buildings, and thus its carbon impact, is attributed to their slabs being the main contributor of weight. Because of their high strength and concrete self-weight reduction, composite beams with hollow-core slabs were created for their technical and economic benefits, making this system inexpensive and with a reduced environmental impact, thereby lowering carbon emissions. Geometrically, the hollow slab has a sequence of T and L form pieces on both sides. Hollow slabs are a newer roof feature with a little study undertaken in mechanical characteristics that prove its benefits and downsides in construction. It also has sufficient rigidity. In this work, numerous 19 hollow slabs and flat slabs are modeled using the finite element method, and the findings are compared in terms of hollow slab behavior and economic cost. It demonstrates that reducing the concrete beneath the hollow slab promotes cost-efficiency and the effective use of concrete and steel resources and various approaches for this form of the hollow slab are provided. Implementing a modern double-side beam slab is possible using the presented methods in this paper. It opens a door for creating structures with high stiffness and strength versus vertical and lateral load, along with low material volume.

Keywords
Hollow core slabs; concrete; simplifying; evaluating; double-side

1. Introduction

Analysis and design of reinforced concrete slabs are two interconnected fields of research. Initially, reinforced concrete floors or slabs were created regularly in the early 20th century. Concrete slabs are one of the most frequent forms of structural components. It is a vertically bounding component of a building [1]. In any panel in the building, the slab element may offer lower support as in (the floor) or upper construction as in (the roof). Slabs are created in various ways, such as pre-cast or composite with various structural systems such as solid, voided, ribbed, and waffle [2]. Concrete floors and roofs are frequently composed of prefabricated hollow core components. These systems are simple to set up and reasonably priced. The depth of the structural members will be reduced to a minimum as a result. The use of longitudinal cores minimizes dead load and results in a more efficient structural structure [3, 4].

In general, structural members must be updated due to a variety of concerns or for special reasons. One of the most typical issues is the requirement for openings to be formed in some circumstances when working with reinforced concrete slabs; the requirement for apertures in slabs is faced in structural engineering. Over the flooring slabs, post-construction elevator or escalator repairs, the installation of new staircases, heat and ventilation ducts, pipeline fire protection, additional skylights, plumbing, air conditioning, benefits (electricity, telephones, and wiring ducts), and architectural aspects are required [5, 6].

HCS (hollow core slab) is a precast or prestressed concrete component with perforations that run the length of the slab, reducing weight and hence cost. Such a lateral advantage might operate in electrical or mechanical management. HCS is mostly used as surface or roof deck systems but may also be used as members, partition sections, and bridge deck elements [7, 8]. Including beams in the hollow slab reduces the dead load compared to a flat slab, the HCS is effective. Slabs are created utilizing dry casting or extrusion molding processes, in which the concrete must be applied extremely thinly using a machine. The concrete is compacted around the cores produced by pipes or roles [9, 10]. The slab with continuous perforations serves as heating/cooling ducts as well as electrical wiring channels. Hollow core slabs reduce sound and vibration transfer between building floors and remove floor squeals [11, 12].

Precast prestressed hollow core (PPHC) flooring is widely used worldwide in multi-story buildings because it is economical, has good sound and heat insulation properties, and provides coverage over a long time. Although PPHC panels exhibit similar performance to other prestressed members in terms of vertical load capacity, span range and deflection control, they are inherently susceptible to failure when considering bending behavior. Brittle due to shear stress [13]. Because web shear failure is the predominant mode of failure in HCS, several studies have been carried out over the years to investigate such a mode of failure [14]. Deeper ceilings with larger spans that must be endured high line loads acting near columns Subject to incipient web shear cracking and failure Less load than expected with legacy code recipe. These shear strengths Reinforcing bar without transverse reinforcement by a detailed non-linear finite element analysis [15].

Mahmoud et al. [16] investigated the behavior of flexural reinforced hollow-core slabs. These slabs were strengthened using an NSM carbon fiber-reinforced polymer strip. Seven full-scale samples were simply supported and subjected to load (monotonic load pattern) till failure. The variables in this study were the utilization of several pre-stressing internal reinforcement ratios as well as three distinct NSM reinforcement ratios. This investigational research focused on failure modes, cracking, deflections, the load-strain relationship, and strengthening capabilities. This study showed that NSM-CFRP strengthening effectively increased the capacity of pre-stressed hollow-core slabs to resist flexural and shear forces.

Teklie et al. [17] presented a study on the shear strength of concrete slabs with longitudinal hollow cores, which included both numerical research and investigative effort. The investigated specimens had diverse hollow core diameters and were tested under various load situations by adjusting the distances of ratios (a/b). The tested specimens were 2.05 m long, 0.6 m wide, and 0.25 m thick. It may demonstrate that load deflection results with each increase in load until the final load that failed with it.

Taskin and Peker [18] developed a numerical finite element simulation of a bi-axial ideal hollow slab form of 8900 mm length, 300 mm width, and 250 mm thickness. This simulation assessed the efficacy of hollow slabs with several hollow forms investigated, including square, spherical, mushroom, and elliptical. The finite element software (LUSAS) performed a non-linear analysis on hollow slabs. That is, to discover the elements that regulate hollow forms, such as shape, corner radius, and diameter, to better understand their impact on slabs, such as crack progressions and their concentration region. A three-dimensional model of a bi-axial hollow form in longitudinal and transversal directions was created using an optimized rectangular slab analysis [19, 20].

In this study, different models of double-side beam slabs and flat slabs were created by varying the height and number of nets. The force-displacement curve of slabs was then obtained in elastic and inelastic regions. In this regard, first and foremost, the finite element model of this slab was created in software, and the properties of the linear behavior of concrete and steel materials were considered. To ensure the accuracy of this modeling, we used the experimental results of the Ibrahim et al. study [21]. Then, force-displacement curves were compared, and a good agreement was observed by changing the number and height of beams. Afterward, the behavior of the double-side beam slab was evaluated in terms of cost-efficiency compared to the flat slab. Finally, a double-side beam slab was proposed due to having simple and cheap implementation. The force-displacement curves were then compared, and a good agreement was observed when the number and height of the beams were changed. Following that, the double-side beam slab's cost-efficiency was evaluated compared to the flat slab. Finally, a double-side beam slab was proposed due to its ease of implementation and low cost.

2. Experimental Model

Several samples of hollow core concrete slabs on a scale of 1:4 with the number and height of a variable net were tested by Abdul-Wahab and Khalil [22]. The dimensions and details of re-baring and loading and abutment conditions of the hollow slab are shown in Figure 1. Moreover, Figure 2 shows typical precast hollow core concrete slabs and some implemented examples. Table 1 presents the main properties of tested specimens by Abdul-Wahab and Khalil [22].

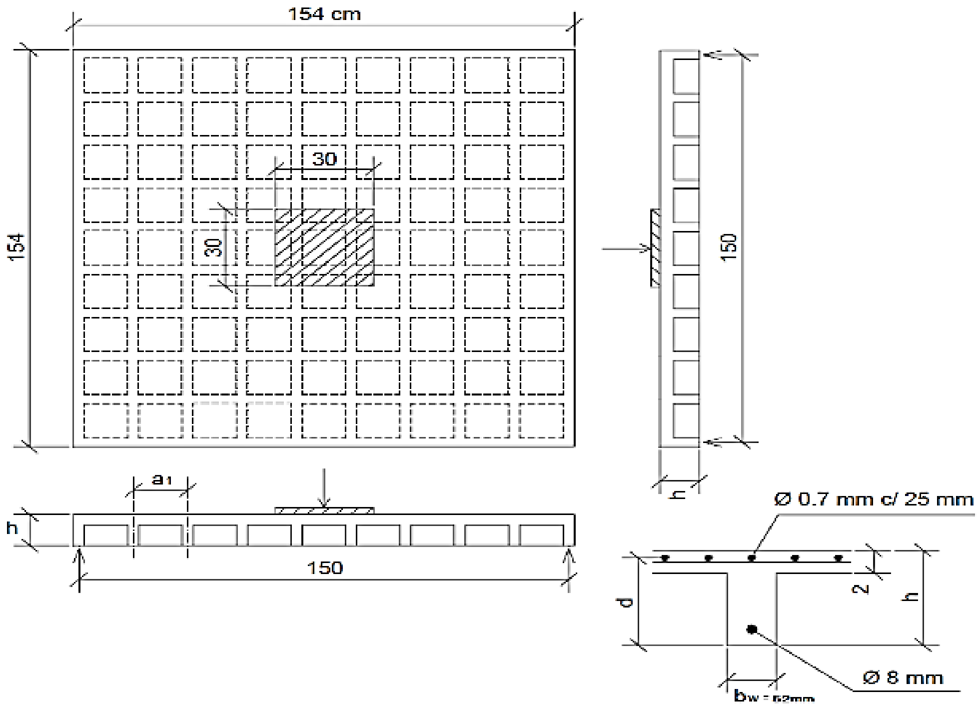

Figure 1 An experimental hollow slab.

Figure 2 Typical precast hollow core concrete slabs (left image) and some implemented examples (middle and right images) adapted from [23, 24].

Table 1 Main properties of the tested specimens by Abdul-Wahab and Khalil [22].

Slab number (1)	Bays (2)	*S* (mm) (3)	*t* (mm) (4)	*W* (mm) (5)	*h* (mm) (6)	*h*/*t* (7)	*A_s* (mm^2/m) (8)
S1	11 × 11	136	20	52	95	4.75	370
S2	9 × 9	167	20	52	95	4.75	301
S3	7 × 7	214	20	52	95	4.75	235
S4	5 × 5	300	20	52	95	4.75	168
S5	9 × 9	167	20	57	125	6.25	301
S6	9 × 9	167	20	47	65	3.25	301
S7	Solid	—	—	—	75	1.00	301
S8	Solid	—	—	—	95	1.00	301

3. Methodology

3.1 Force-displacement Behavior of Hollow Slab

For investigation of the hollow slab behavior, the analysis of the slab using the plate theory method [25], can be a complicated and time-consuming method:

$$D_x \frac{\partial^4 w}{\partial x^4} + 2\mathrm{H} \frac{\partial^4 w}{\partial x^2 \, \partial y^2} + D_y \frac{\partial^4 w}{\partial y^4} = \mathrm{q} \tag{1}$$

In which, q is the load on the slab, $\mathrm{D_x}$ and D_y are the flexural rigidity of the slab in the longitudinal and transverse directions which are proposed for the practical applications by following relations:

$$\mathrm{D_x} = \frac{\mathrm{EI_{sx}}}{\mathrm{s_x}} \tag{2}$$

$$\mathrm{D_y} = \frac{\mathrm{EI_{sy}}}{\mathrm{s_y}} \tag{3}$$

Where I_{sx} and I_{sy} are the moments of inertia of the cross-section relative to the neutral axis in the x and y directions. Also, s_x and s_y are the distance between the nets perpendicular to x and y axes. 2H is the torsional rigidity of the hollow slab which is computed as below concerning Figure 3:

$$2\mathrm{H} = \mathrm{B_{xy}} + \mathrm{B_{yx}} + \frac{\mathrm{Et^3}}{6(1-\xi^2)} + \frac{\xi \mathrm{E}}{2} . \frac{\mathrm{W_x . W_y}}{\mathrm{s_x s_y}} (\mathrm{h_y} - \mathrm{t}) \times \left[(\mathrm{h_y} - \mathrm{t})(\mathrm{h_y} - \mathrm{t}) - (\mathrm{e_x} + \mathrm{e_y}) + \frac{(\mathrm{h_y} - \mathrm{t})^2}{3} \right] \tag{4}$$

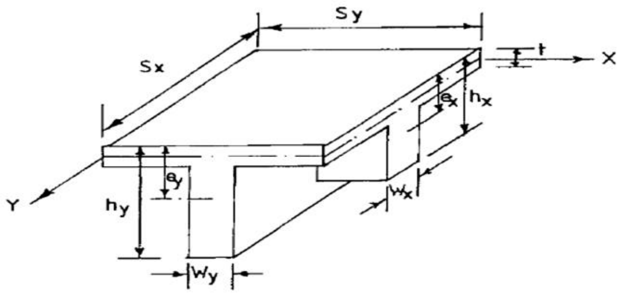

Figure 3 The cross section of the perpendicular network.

B_{xy} and B_{yx} are the rigidity of nets in the longitudinal and transverse directions which are computed as follows:

$$B_{xy} = \frac{6KW_x{}^3(h_x - t)}{s_x} \quad \text{for} \quad W_x < (h_x - t) \tag{5}$$

$$B_{yx} = \frac{6KW_y{}^3(h_y - t)}{s_y} \quad \text{for} \quad W_y < (h_y - t) \tag{6}$$

The third expression of equation 4 represents the torsional stiffness of the slab deck, while the fourth expression is connected to the Poisson factor, ξ is caused by net contact. In an approximation analysis, the fourth expression of this equation is negligible. It should be emphasized that all preceding relations only apply to the elastic area.

4. Numerical Simulation

A simulation software (ABAQUS) was used to model slabs using the finite element method for complex analyses like nonlinear or dynamic analysis [26]. A finite element software typically consists of three major components: 1) model creation, 2) loading and analysis, and 3) observing results. It should be noted that four simple abutments supports the slab model. The plastic damage model was used to define the nonlinear behavior of concrete [26]. Table 2 shows the used properties in FEM for steel and concrete.

Table 2 Steel and concrete properties in FEM.

Type of element	Poisson coefficient	Elastic modulus
Steel	0.3	210000 N/mm^2
Concrete	0.18	18000 N/mm^2

Because of the presence of nets and their complexity, a three-dimension three-node Tet (C3D4) element was used [27, 28]. Because it is stiffer than the other elements. A two-node truss element (T3D2) was used to mesh a steel model. In the preliminary analysis, the mesh density was chosen uniformly. However, the responses were not more accurate. Because the size of the concrete mesh is important in the accuracy and speed of calculations in the finite element method, the density of the mesh was increased below the loading region and gradually decreased towards the edges to achieve high accuracy and speed in calculations at the same time. In addition, the displacement change of loading is applied in this model due to loading on a rigid plate in the laboratory (Figure 4).

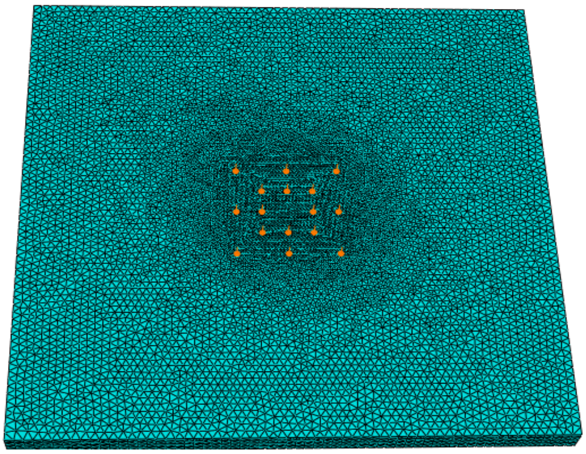

Figure 4 The surface on the hollow slab of finite element and loading region.

5. Verifications

5.1 Analytical Verification

To validate this modeling and analysis, the analysis results were compared with the experimental results for hollow slab $\boldsymbol{S_1}$. This slab has 12 nets with a height of 75 and a width of 52 mm in every direction and a reinforced slab with 20 mm thickness has been performed on it.

5.2 Numerical Verification

To investigate the behavior of specimens, three-dimensional FE models have been created using the Simulia Abaqus. As you see in Figure 5 and Figure 6, the numerical model shows good accuracy relative to the experimental model. Both models entered to cracking region at almost 30 kN. So, the preliminary cracks appeared in them, showing a final strength of almost 105 kN. The surface underneath the slab has been cracked on the central part towards the edges in both samples [29].

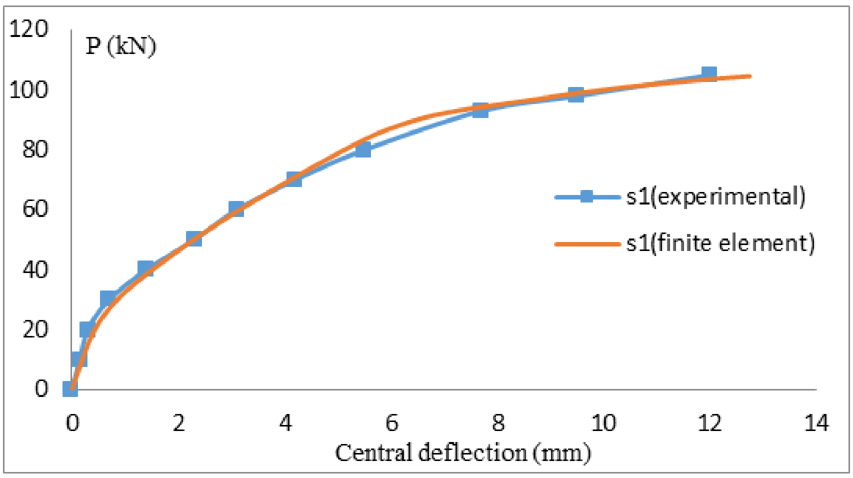

Figure 5 The displacement of the $\boldsymbol{S_1}$ slab center.

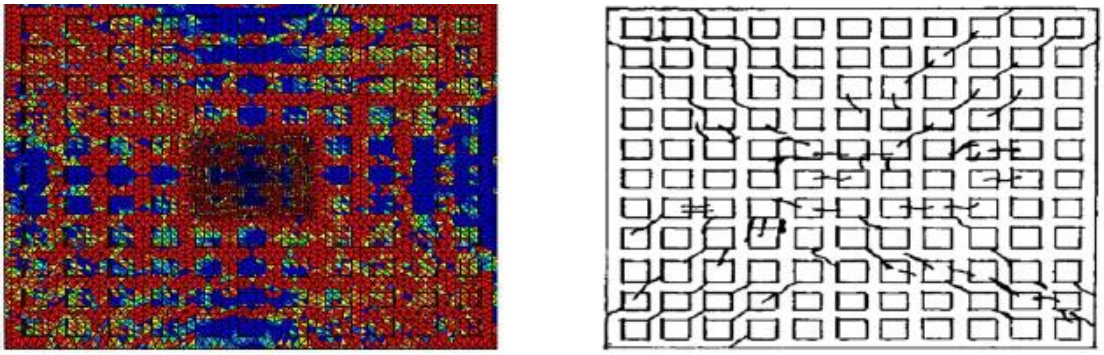

Figure 6 The cracking location of the $\boldsymbol{S_1}$ experimental hollow slab and its finite element model.

6. Results and Discussion

6.1 The Effect of Net Number on the Stiffness and Strength of a Double-sided Beam Slab

Here, two types of hollow slabs including $S_1(two\ ways)$ and $S_4(two\ ways)$ have been modeled. They have 12 and 6 nets in each direction with a height of 95 and a width of 52 mm, respectively.

As it is shown in Figure 7, the increase in the number of nets has a slightly low impact on the elastic strength of the slab, so that elastic strength reaches from 20 kN in $S_4(two\ way)$ with 6 nets to 30 kN in $S_1(two\ ways)$ with 12 nets for each direction. However, the final strength ranges from 50 kN in $S_4(two\ ways)$ to 105 kN in $S_1(two\ ways)$. It shows that the number of nets has too much impact on final strength. The diagram of Figure 7 shows that as the number of nets increases, the stiffness increases and the ductility decreases due to the limited final displacement of slabs.

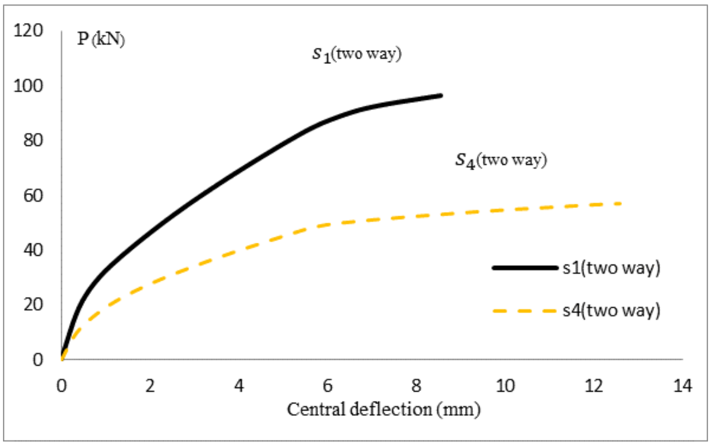

Figure 7 Comparison of force-displacement diagrams of $S_1(two\ ways)$ and $S_4(two\ ways)$.

6.2 The Effect of the Double-side Beam Slab's Stiffness and Strength

To show the height impact of nets on the stiffness and strength of hollow slabs, a $S_5(two\ ways)$ model with a net number equal to $S_4(two\ ways)$, i.e., 6, in each direction, and a net height twice that the $S_4(two\ ways)$, i.e., 125 mm in height, with 57 in mm width and equal rebar value is considered.

The diagram in Figure 8 shows that twice the net slab height causes the cracking strength and final strength to increase from almost 20 kN and 50 kN in $S_4(two\ ways)$ to over twice, i.e., 55 kN and 140 kN in $S_5(two\ ways)$, respectively. It is noted that when the stiffness and strength increase, the slab has lower ductility and the probability of sudden failure (shear failure) is higher in it. Because this failure is brittle and sudden, bending failure occurs ductile.

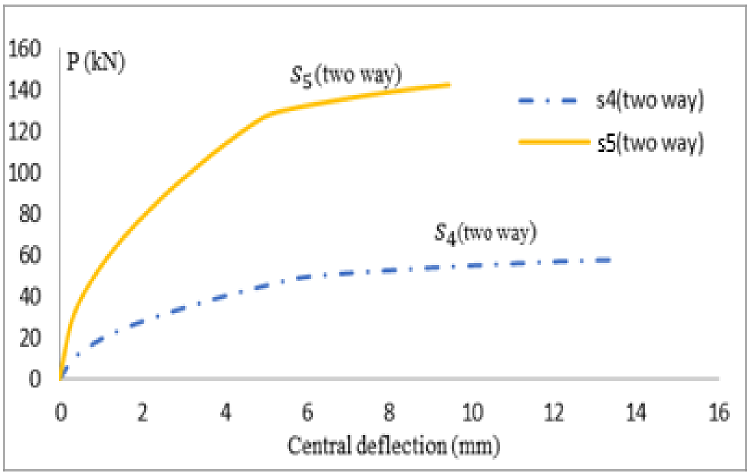

Figure 8 Comparison of force-displacement diagrams of $S_4(two\ ways)$ and $S_9(two\ ways)$.

6.3 The Effect of Height on the Volume of Concrete and Rebar in a Double-sided Beam Slab

The impact of net height and net numbers are compared in terms of stiffness and strength for a case where the volume of concreting and that of rearing are considered equal. For this purpose, $S_1(two\ ways)$ and $S_5(two\ ways)$ that their volume of concrete and that of rebar are equal to each other, are analyzed.

The diagram of Figure 9 shows that crack stiffness and strength of the $S_5(two\ ways)$ and final strength are more than $S_1(two\ ways)$. It means that in the double-side beam slabs for an equal amount of concrete and steel, the impact of a higher height increase is more than that of the beam number increase. But, $S_5(two\ ways)$ has less ductility than $S_1(two\ ways)$ because of its same final displacement, so the possibility of sudden failure is more in them.

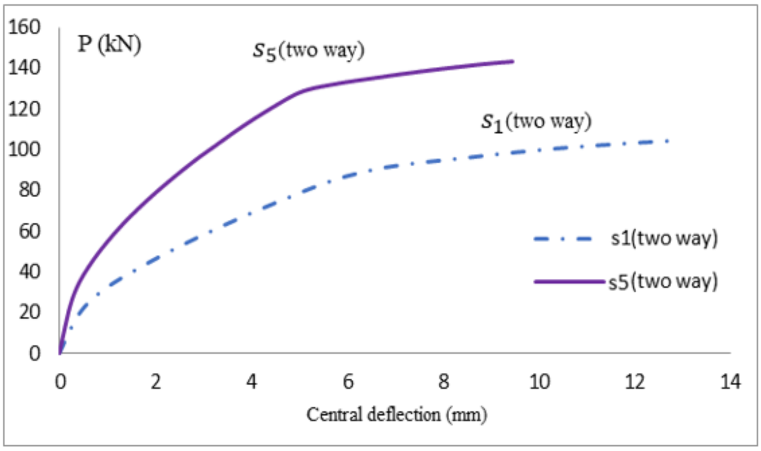

Figure 9 Comparison of force-displacement diagrams of $S_1(two\ ways)$ and $S_9(two\ ways)$.

6.4 Evaluation of the Equivalent Thickness Method and Economic Comparison with Flat Slab

The equivalent thickness is equal to the thickness of the flat slab. It has the same flexural stiffness as a double-side beam slab. To evaluate it, $S_2(two\ ways)$, which has 10 nets with a height of 75 mm and width of 52 mm in each direction and on which a 20 mm reinforced slab is performed, is considered as the base slab, and $S_7(flat\ slab)$ flat slab is obtained with a 75 mm thickness. This thickness equals the equivalent thickness of $S_2(two\ ways)$ calculated as follows [30].

$$h_e = \left(\frac{12I}{S}\right)^{1/3} \tag{7}$$

The diagram of Figure 10 verifies the equivalent thickness method. This equivalent thickness can be used for ease of analysis and design. It is noted that the $S_2(two\ ways)$ hollow slab has approximately equal bending stiffness and higher strength than the $S_7(flat\ slab)$ flat slab. Also, the concrete volume will be reduced by almost 19%, which shows the economic efficiency of this type of slab compared to a flat slab.

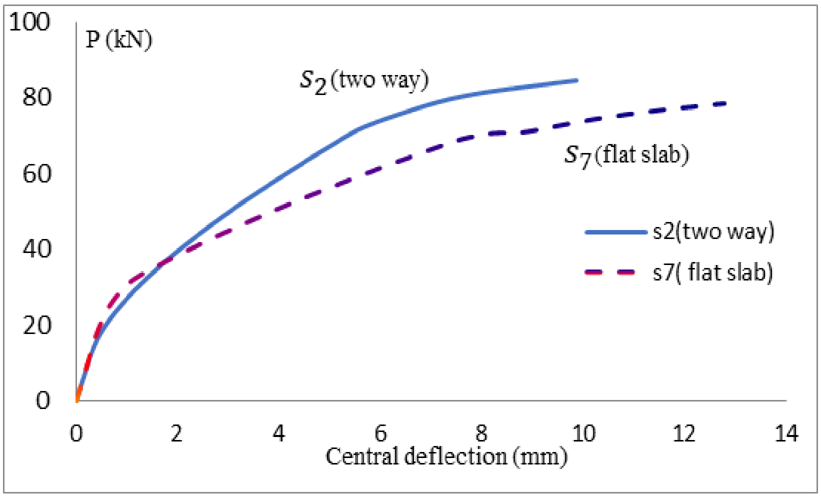

Figure 10 Comparison of force-displacement diagrams of $S_2(two\ ways)$ and $S_7(flat\ slab)$.

6.5 Modern Method of the Double-side Beam Slab

Due to problems such as the lack of a manufacturing plant, the production of some prefabricated molds, the high initial cost of molding, and the lack of expertise, implementing the hollow slab is not cost-efficient. So, we present possible mechanisms to facilitate the implementation of such slabs. It will be a useful step to achieve this goal in the year of national production (Figure 11). It calls the modern method due to the novel design philosophy and a novel implementation method of this double-side beam. When the structure is subjected to a minor earthquake, the joint remains elastic without any damage. When the structure is subjected to a moderate earthquake, the joint has a satisfactory self-centering effect, and is accompanied by an appropriate energy consumption [31].

Figure 11 Modern implementation of the hollow slab.

6.6 A Simple Method Like Flat Slab

In this method, wooden, metal, and plastic molds can be used underneath molds like a double-sided flat slab.

To make this type of roof, piling is done at intervals of 1 to 1/2 m under the roof and four wooden chips and molds are placed on them. After fixing the formwork, reinforcement of nets is done. In order to make a hollow slab and reduce the weight of concrete, existing blocks, especially polystyrene (iolite) blocks, are used instead of prefabricated blocks due to their lightweight. So that after molding under the slab and repairing, the blocks are placed between rebars and on the formwork. Then, concreting is done. It is noted that after the concrete stuck and the following formwork was removed, the blocks could be separated from the slab (Figure 12).

Figure 12 The implementation of the slab in laboratory on a small scale.

6.7 Using In-place, Prefabricated and Chromite Beams

The implementation of the in-place method requires much more accuracy and patience. Nevertheless, this method is simple and cheap. First, the wooden or metal plates of the beams are properly connected to the boundary beams after being stacked in one direction to avoid lateral movement. Note that the panel width must be greater than the beam thickness at this stage. This allows for easy placement of secondary beam blocks and forms perpendicular to the panel [32, 33].

According to Figure 13, wooden or metal small molds of secondary beams in the form of U, with a width equal to the beam width and a length equal to the distance between the nets, are placed on the primary beam molds. Keeping these molds fixed is a little difficult due to their small size. It is recommended that if a wooden mold is used, the four-chip small rectangular wood can be connected to the primary beams' wooden to prevent secondary mold movement. , If metal molds are used, they must be made so steel clamps can hold in place [34].

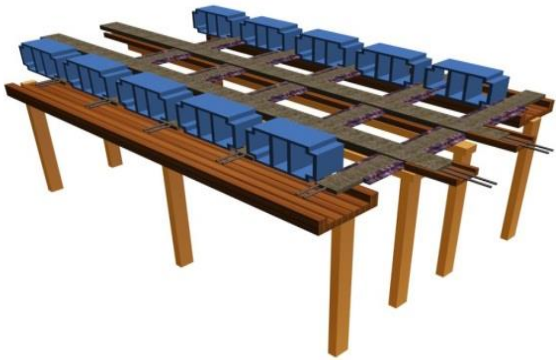

Figure 13 Using an in-place beam on both sides.

Using an in-place beam in one direction can be applied and implemented easily. Compared to other methods, an important benefit of this method is that prefabricated beams are used on one side, which can reduce the volume of executive operations and the cost of molding [35].

If the vertical rebars can pass through the prefabricated beams, after passing them, rectangular molds will be closed under the beams and after placing the blocks, concreting is performed by Figure 14. Suppose we cannot pass vertical rebars through the beams due to rebar diameter, inflexibility, or performance issues. In that case, rebars can be wire-connected to prefabricated beams, and U-shape wooden or metal molds can be located below them at a suitable height. After placing the blocks, the concrete is poured. In addition, when constructing the main girder formwork with the U-shaped timber and metal formwork, the height of the main girder formwork should be lower than the height of his U-formwork so that the reinforcing bars pass through the concrete. Composite can be realized. Disadvantages of this method include the relief created by molding under the slab. This creates an architectural and visual problem under the slab that joinery can easily remove (Figure 14).

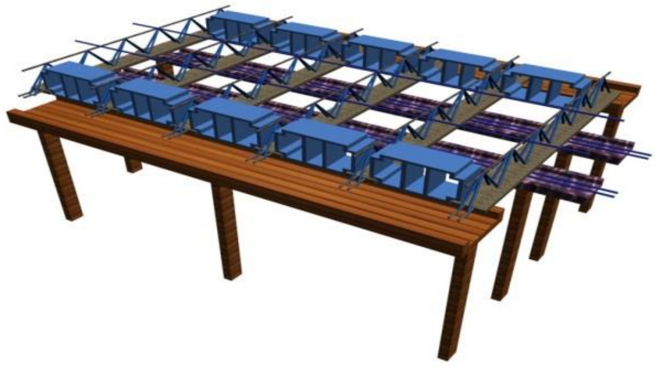

Figure 14 Using in-place beams on one side and prefabricated beams on the other side.

This method can be the best because it has all the advantages of a one-side chromite beam roof, such as no need for pilling [36], simultaneous implementation of several roofs, lateral stiffness of many floors, and all the advantages of a double-side beam slab. First, a prefabricated chromite beam is on one side [37]. Sheets with a thickness and width equal to the lower sheets of a prefabricated chromite beam should be welded to it or a whole sheet should be used.

In a direction perpendicular to the prefabricated chromite beam, if necessary, compression rebar or steel sheet is located in the upper part and concreting is done (Figure 15).

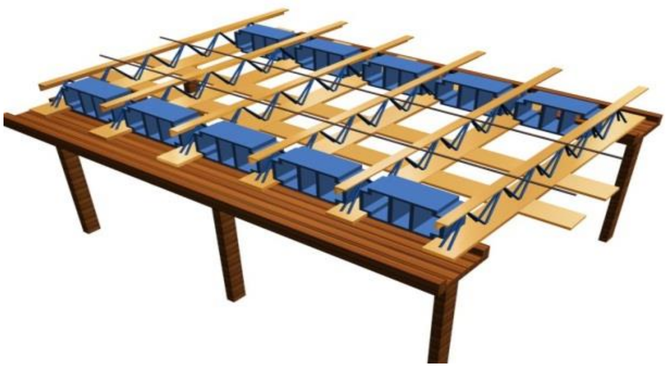

Figure 15 Using a chromite beam.

7. Conclusions

In this study, numerical analysis was performed and compared to experimental results in order to evaluate the performance of hollow core slabs (HCS)-concrete and simplify their implementation, and the following conclusions were reached:

- In double-side beam slabs under vertical load, the impact of height increases on the stiffness increase and strength increase is more than the impact of the beam number increase.
- A double-side beam slab is more likely to have higher height shear failure.Twice the net slab height in finite element causes the cracking strength. When the stiffness and strength increase, the slab has lower ductility and the probability of sudden failure (shear failure) is higher. Because this failure is brittle and sudden, bending failure occurs ductile.
- Regarding numerical simulation, the increase in the number of nets has a slightly low impact on the elastic strength of the slab, but it has too much impact on the final strength.

- According to numerical results, All the HCS remain uncracked at design service loads indicating the superior serviceability performance of the HCS.
- The double-side beam slab with bending stiffness approximately equal to or higher than the flat slab considerably reduces the volume of concreting.
- It shows that the double-side beam slab is more cost-efficient and stronger than the flat slab.
- Implementing a modern double-side beam slab in some countries is not cost-efficient due to a lack of plants for manufacturing prefabricated molds, and it has a relatively high cost.
- The implementation of a modern double-side beam slab is possible using the presented methods in this paper and opens a door for creating structures with high stiffness and strength versus vertical load and lateral load, along with low material volume.

Author Contributions

All authors have equal contributions.

Competing Interests

The authors have declared that no competing interests exist.

References

1. Yousefi A, Bunnori NM, Khavarian M, Hassanshahi O, Majid TA. Experimental investigation on effect of multi-walled carbon nanotubes concentration on flexural properties and microstructure of cement mortar composite. AIP Conf Proc. 2017; 1892: 020032.
2. Al-Shaarbaf IA, Al-Azzawi AA, Abdulsattar R. A state of the art review on hollow core slabs. ARPN J Eng Appl Sci. 2018; 13: 3240-3245.
3. Stanton JF. Response of hollow-core slab floors to concentrated loads. PCI J. 1992; 37: 98-113.
4. Abedi M, Hassanshahi O, Rashiddel A, Ashtari H, Meddah MS, Dias D, et al. Investigation of mechanical behavior of a sustainable cementitious composite reinforced with natural fibre: An experimental and numerical study. 2022. doi: 10.2139/ssrn.4247583.
5. Mohamed OA, Kewalramani M, Khattab R. Fiber reinforced polymer laminates for strengthening of RC slabs against punching shear: A review. Polymers. 2020; 12: 685.
6. Hassanshahi O, Majid TA, Lau TL, Yousefi A, Tahara RM. Seismic performance of the typical RC beam–column joint subjected to repeated earthquakes. AIP Conf Proc. 2017; 1892: 120014.
7. Mahdi AA, Ismael MA. Structural behavior of hollow-core one way slabs of high strength self-compacting concrete. Int J Eng. 2021; 34: 39-45.
8. Peen WY, Keong CK, Hassanshahi O. Behaviour of hollow circular section with multiple perforations under compression, flexure and torsion. Lat Am J Solids Struct. 2019; 16: e169.
9. Alobaidy QN, Abdulla AI, Al-Mashaykhi M. Shear behavior of hollow ferrocement beam reinforced by steel and fiberglass meshes: Shear behavior. Tikrit J Eng Sci. 2022; 29: 27-39.
10. Abdulla AI, Khatab HR. Behavior of multilayer composite ferrocement slabs with intermediate rubberized cement mortar layer. Arab J Sci Eng. 2014; 39: 5929-5941.
11. Frankl B, Lucier G, Rizkalla S, Blaszak G, Harmon T. Structural behavior of insulated prestressed concrete sandwich panels reinforced with FRP grid. Proceedings of the Fourth International

Conference on FRP Composites in Civil Engineering (CICE2008); 2008 July 22-24; Zurich, Switzerland. Champs-sur-Marne: RILEM Association.
12. Salati M, Bragança L, Mateus R. Sustainability assessment on an urban scale: Context, challenges, and most relevant indicators. Appl Syst Innov. 2022; 5: 41.
13. Sarkis AI, Sullivan TJ, Brunesi E, Nascimbene R. Critical modelling criteria for precast pre-stressed hollow-core slabs. J Build Eng. 2022; 54: 104545.
14. Brunesi E, Nascimbene R. Numerical web-shear strength assessment of precast prestressed hollow core slab units. Eng Struct. 2015; 102: 13-30.
15. Brunesi E, Bolognini D, Nascimbene R. Evaluation of the shear capacity of precast-prestressed hollow core slabs: Numerical and experimental comparisons. Mater Struct. 2015; 48: 1503-1521.
16. Mahmoud K, Foubert S, El-Salakawy E. Strengthening of prestressed concrete hollow-core slab openings using near-surface-mounted carbon-fiber-reinforced polymer reinforcement. PCI J. 2017; 62: 45-57.
17. Teklie M, Alemu T, Benti B. Behaviors of reinforced concrete slab voided by circular paper tubes. Eng Sci. 2020; 5: 45-56.
18. Taskin K, Peker K. Design factors and the economical application of spherical type voids in RC slabs. Proceedings of the International Scientific Confrence People, Buildings and Environment; 2014 October 15-17; Kroměříž, Czech Republic. pp. 448-458.
19. Oh CL, Choong KK, Nishimura T, Kim JY, Hassanshahi O. Shape change analysis of tensegrity models. Lat Am J Solids Struct. 2019; 16: e221.
20. Chung JH, Park JH, Choi HK, Lee SC, Choi CS. An analytical study on the impact of hollow shapes in bi-axial hollow slabs. Proceedings of the FraMCoS-7; 2010 May 23-28; Jeju Island, Korea. Seoul: Korea Concrete Institute. pp. 1729-1736.
21. Ibrahim IS, Elliott KS, Abdullah R, Kueh AB, Sarbini NN. Experimental study on the shear behaviour of precast concrete hollow core slabs with concrete topping. Eng Struct. 2016; 125: 80-90.
22. Abdul-Wahab HM, Khalil MH. Rigidity and strength of orthotropic reinforced concrete waffle slabs. J Struct Eng. 2000; 126: 219-227.
23. Larbi JA, Siemes AJ, Polder RB. Exposed to fire. In: Tailor made concrete structures. Boca Raton, FL: CRC Press; 2008. p. 132.
24. Xu X, Yu J, Wang S, Wang J. Research and application of active hollow core slabs in building systems for utilizing low energy sources. Appl Energy. 2014; 116: 424-435.
25. ACI Committee. Building code requirements for structural concrete (ACI 318-05) and commentary (ACI 318R-05). Farmington Hills, MI: American Concrete Institute; 2004; ACI 318-05.
26. Ahmed A. Modeling of a reinforced concrete beam subjected to impact vibration using ABAQUS. Int J Civ Struct Eng. 2014; 4: 227-236.
27. Nascimbene R. Penalty partial reduced selective integration: A new method to solve locking phenomena in thin shell steel and concrete structures. Curved Layer Struct. 2022; 9: 352-364.
28. Hippola HM, Wijesundara KK, Nascimbene R. Response of shear critical reinforced concrete frames and walls under monotonic loading. En Struct. 2022; 251: 113483.

29. Wang W, Zhang D, Lu F, Wang SC, Tang F. Experimental study and numerical simulation of the damage mode of a square reinforced concrete slab under close-in explosion. Eng Fail Anal. 2013; 27: 41-51.
30. Yu J, Tan KH. Structural behavior of reinforced concrete frames subjected to progressive collapse. ACI Struct J. 2017; 114: 63-74.
31. Dongde S, Yong Y, Yinke M, Yicong X, Yunlong Y, Shiqiang F. Experimental study on seismic performance of prefabricated replaceable beam-column connectors using double-sided angle steel. J Build Eng. 2022; 51: 104095.
32. Mahboob A, Gil L, Bernat-Maso E, Eskenati AR. Flexible fiber fabric for FRP–concrete connection of thin hybrid slabs. Polymers. 2021; 13: 2862.
33. Abbasi S, Mahboob A, Bakhtiari Zamani H, Bilesan MR, Repo E, Hakimi A. The tribological behavior of nanocrystalline TiO_2 coating produced by plasma electrolytic oxidation. J Nanomater. 2022; 2022: 5675038.
34. Eskenati AR, Mahboob A, Bernat-Maso E, Gil L. Experimental and numerical study of adhesively and bolted connections of pultruded GFRP I-shape profiles. Polymers. 2022; 14: 894.
35. Sima JF, Roca P, Molins C. Cyclic constitutive model for concrete. Eng Struct. 2008; 30: 695-706.
36. Malviya S, Tiwari MV. Behaviour of flat slab, waffle slab, ribbed & secondary beam in a multistorey building under seismic response: A review. Int J Res Appl Sci Eng Technol. 2020; 8: 986-992.
37. Kwak HG, Kim DY. Material nonlinear analysis of RC shear walls subject to monotonic loadings. Eng Struct. 2004; 26: 1517-1533.